RESEARCH ARTICLE | AUGUST 28 2025

Development of a capacitance measurement for pulsed magnetic fields

William K. Peria ; Shengzhi Zhang ; Sangyun Lee ; Gabriel Silva Freitas ; Vivien S. Zapf ;
Choongjae Won ; Sang-Wook Cheong ; Minseong Lee ✉

Check for updates

CHORUS

View Online

Export Citation

AIP Publishing

Development of a capacitance measurement for pulsed magnetic fields

View Online   Export Citation   CrossMark
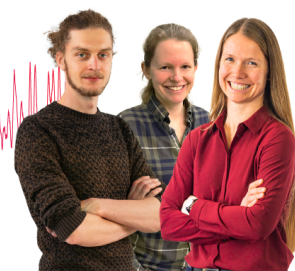
William K. Peria,[1,a] (iD) Shengzhi Zhang,[1] (iD) Sangyun Lee,[1] (iD) Gabriel Silva Freitas,[1] (iD) Vivien S. Zapf,[1] (iD) Choongjae Won,[2] (iD) Sang-Wook Cheong,[3] (iD) and Minseong Lee[1,b] (iD)

AFFILIATIONS

[1] National High Magnetic Field Laboratory, Los Alamos National Laboratory, Los Alamos, New Mexico 87545, USA

[2] Laboratory for Pohang Emergent Materials and Max Planck POSTECH Center for Complex Phase Materials, Department of Physics, Pohang University of Science and Technology, Pohang 37673, Republic of Korea

[3] Keck Center for Quantum Magnetism and Department of Physics and Astronomy, Rutgers University, Piscataway, New Jersey 08854, USA

[a] **Present address:** National Institute of Standards and Technology, Boulder, CO 80305, USA. william.peria@nist.gov
[b] **Author to whom correspondence should be addressed:** ml10k@lanl.gov

ABSTRACT

Capacitance measurements are crucial for probing the electrical properties of materials. In this study, we develop and implement a capacitance measurement technique optimized for pulsed magnetic fields. Our approach employs an auto-balancing bridge method, leveraging a high-bandwidth transimpedance amplifier to mitigate parasitic contributions from coaxial cables. This technique enables precise capacitance measurements in rapidly changing magnetic fields, as demonstrated in experiments on the magnetoelectric material $NiCo_2TeO_6$. The results reveal strong magnetoelectric coupling, including a pronounced hysteresis in capacitance that coincides with magnetization measurements and an enhanced energy dissipation peak at high sweep rates. Compared to traditional LCR meter measurements in DC fields, our method exhibits excellent agreement while providing additional insight into field-induced phase transitions. This work establishes a robust methodology for capacitance measurements under extreme conditions and opens new opportunities for studying multiferroic and correlated electron systems under high magnetic fields.

I. INTRODUCTION

Capacitance measurements are a foundational aspect of modern scientific research and material studies, playing a critical role in deepening our understanding of both natural and engineered materials. The capacitance of the materials provides invaluable insights into the fundamental material properties, such as the dielectric constant and loss factor, which are key to the development of innovative materials and devices. Furthermore, the capacitance measurement technique can also be extended to other measurements, for example, capacitive thermometry,[1,2] capacitive torque magnetometry,[3] and capacitive dilatometry,[4] to name a few. For these reasons, the capacitance measurement is employed by research and engineering laboratories across the world.

In the study of material properties, researchers investigate the response of materials by varying external parameters. Common external parameters include temperature, pressure, and magnetic fields. Among these, magnetic fields couple to magnetic materials rather weakly, requiring high magnetic fields to control the properties of materials.[5–9] Following the research trend of demanding increasingly strong magnetic fields, efforts in high magnetic field studies are focused on developing magnets capable of generating even higher fields.[10–12]

One method to achieve high magnetic fields is the use of pulsed magnetic fields.[13] Simply put, pulsed magnetic fields are generated by releasing the energy stored in a capacitor bank into a solenoid electromagnet over a very short period, creating an extremely high magnetic field. For instance, the 65 T short pulse magnet most
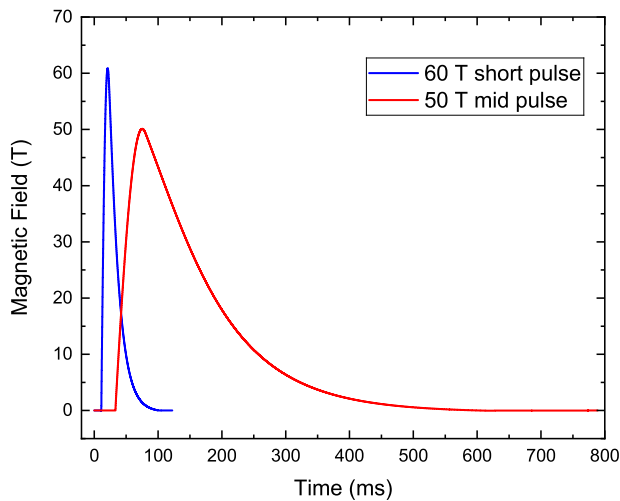
30 September 2025 18:22:38

FIG. 1. Time-dependent magnetic field profiles of the short-pulse and mid-pulse magnets at the National High Magnetic Field Laboratory, Los Alamos National Laboratory.

commonly used at the National High Magnetic Field Laboratory located at the Los Alamos National Laboratory reaches its maximum field from 0 T in 8.5 ms and then rapidly decays back to 0 T over 100 ms. A slower mid-pulse magnet can reach up to 59 T, operating approximately five to six times more slowly than the short pulse magnet [see Fig. 1(a)]. The details of the magnets can be found in Refs. 14–16.

In such ultra-fast environments, commercially available capacitance bridges or LCR meters cannot be used. This limitation arises because their measurement speeds are restricted to several milliseconds due to the time required for bridge balancing and data averaging, which makes them clearly incompatible with the timescales of the pulsed fields described above. As a result, these attempts are very rare. One method utilizes a commercial general radio (GR) capacitance bridge, where the bridge is balanced prior to the measurement, and the unbalanced signal is then used for the measurement.[17] While this allows for very accurate capacitance measurements, there are several drawbacks. Not only has the production of GR bridges been discontinued but also their maximum operating frequency is limited to 100 kHz, making it difficult to measure capacitance at higher frequencies. In addition, this limitation of the frequencies makes it difficult to experiment with relatively faster short pulse magnets. Finally, if a phase transition occurs and the capacitance is divergent, the unbalanced signal deviates from a linear relationship requiring additional data processing for precise quantification.

In this paper, we employ the so-called auto-balancing bridge method, which leverages the high-quality virtual ground at the input of a transimpedance amplifier to measure capacitance in rapidly changing environments using transport measurement techniques. The primary challenge in capacitance measurements via transport techniques arises from the coaxial cable, which is connected in parallel with the sample. Consequently, the measured capacitance includes contributions from both the sample and the coaxial cable. While the sample capacitance is typically only a few picofarads (pF), a 1 m coaxial cable can contribute several hundred pF, making it

challenging to extract the sample signal accurately. As detailed later, connecting the sample to a virtual ground eliminates any potential difference between the inner and outer conductors of the coaxial cable. This eliminates parasitic contributions from the capacitance of the cables and enables precise detection of the AC current flowing through the sample.

II. CAPACITANCE MEASUREMENTS IN CRYOSTATS AND PULSED-FIELD MAGNETS

To measure the capacitance of the device under test (DUT) at low temperatures and in high magnetic fields, we employ a custom-built probe with the sample positioned at its end. Shielded coaxial cables are used for both excitation voltage and signal detection to minimize external noise. The residual capacitance of these cables is represented in Fig. 2 as C_{HI} for the cable connecting the excitation voltage to the DUT and C_{LO} for the cable linking the DUT to the signal measurement station. The capacitance of these coaxial cables typically ranges from a few tens to several hundred pF, which can be up to two orders of magnitude larger than that of many DUTs.

A. Oscillating voltage source

An analog AC voltage with a sinusoidal waveform V_{in}, generated by a function generator with negligible output impedance, operates at 101 kHz with an RMS amplitude of 0.5 V [Fig. 3(a)]. This signal is fed into a commercially available voltage amplifier (Advanced Energy, Trek 2100HF, denoted as Voltage Amplifier 1 in Fig. 2), which has an input impedance of R_{ai} of 50 Ω. The signal is amplified by a factor of 50 to achieve a high signal-to-noise (S/N) ratio.

The excitation frequency is chosen to be sufficiently high to ensure an adequate number of data points are collected within the rise time of the field pulse while remaining below the capacitor's
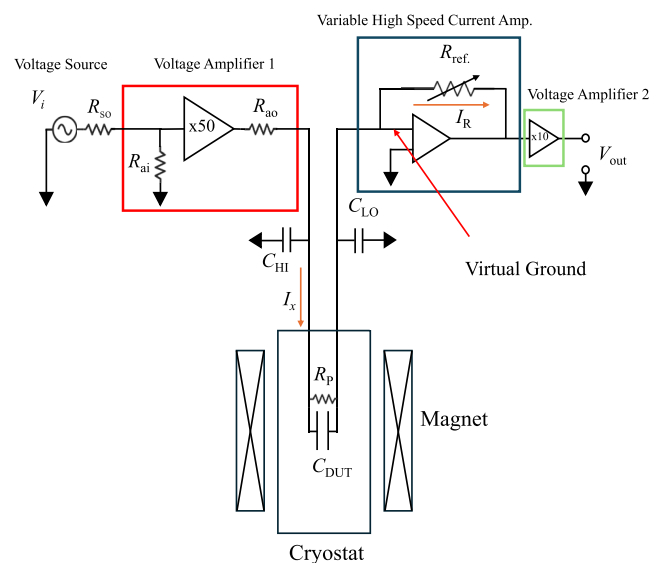
FIG. 2. Overview of the circuit for the capacitance measurement system in a pulsed magnetic field presented in this paper.
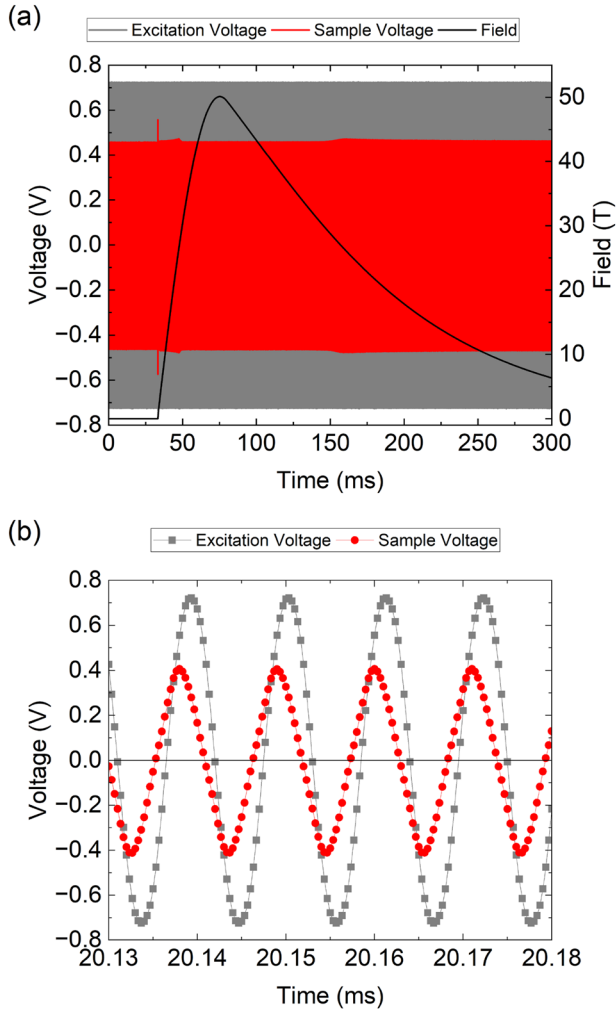
(a)

(b)

FIG. 3. (a) Excitation voltage (gray dots) and sample signals (red dots) as functions of time, recorded by the digitizer, along with the magnetic field strength as a function of time (black curve). (b) Enlarged view of the pre-trigger region from (a).

self-resonant frequency (SRF) to prevent parasitic inductance from dominating the signal. For instance, with a parasitic inductance of 1 nH (typical for a ceramic capacitor) and a capacitance of 1 pF, the SRF is in the GHz range. We assume that these components are in series, which is reasonable given that the inductance mainly originates from wiring and electrode structures within the DUT. The total impedance is ~1.6 MΩ at the frequency chosen in this paper; the capacitive impedance is ~1.6 MΩ; and the inductive impedance is only about 600 $\mu\Omega$—many orders of magnitude smaller. This confirms that inductive effects are negligible at this frequency, and the measured impedance reliably reflects the DUT's capacitance. However, the frequency can be adjusted as needed as far as the frequency is well below the SRF and within the bandwidth of the amplifier.

In addition, the timescale of the chosen excitation frequency is much longer than the RC time constant determined by the

capacitance of the DUT and the reference resistor R_{ref} in the variable high-speed current amplifier.

B. Auto-balancing bridge

A commercial high-bandwidth transimpedance amplifier (TIA) [variable gain high speed transimpedance amplifier (current amplifier) DHPCA-100, FEMTO®] is directly connected to the DUT, with its gain optimized based on the excitation frequency, typically around 10^3 Ω. We chose this value for two reasons: first, it provides a larger signal that facilitates signal processing; more importantly, the time constant—determined by the capacitance of the DUT and this resistance—is ~3 ns, which is much shorter than the timescales associated with the frequencies used in this study. TIA's input is held at a virtual ground, ensuring the current through the sample (I_x in Fig. 2) equals the current through the range resistor (I_R in Fig. 2), thereby eliminating parasitic contributions from coaxial cables C_{LO} in the capacitance measurement.[18] The TIA output is fed to a commercially available voltage amplifier (SR 560, Stanford Research Systems, denoted as Voltage Amplifier 2 shown in Fig. 2) to increase the S/N ratio by amplifying and filtering the signal.

C. Voltage detection

The output voltage of Voltage Amplifier 2, V_{out}, and the input voltage, V_{in}, are recorded simultaneously using a high-bandwidth digitizer from National Instruments. These measured values are then used to calculate the complex impedance of the DUT, Z_{tot}, according to

$$Z_{tot}^{-1} = \frac{1}{R_{ref}} \frac{V_{out}}{V_{in}} \tag{1}$$

$$= |Z_{tot}^{-1}| \exp(i\phi) . \tag{2}$$

In the frequency range of interest, the impedance of the DUT is on the order of 1 MΩ. It is, therefore, appropriate to determine the capacitance of the sample by modeling it as a parallel resistor-capacitor circuit,

$$Z_{tot}^{-1} = i\omega C_{DUT} + \left(\frac{1}{R_P}\right). \tag{3}$$

By solving for the capacitance and resistance, we obtain the following:

$$C_{DUT} = \left|\frac{Z_{tot}^{-1}}{\omega}\right| \sin\phi, \tag{4}$$

$$R_P = \frac{1}{|Z_{tot}^{-1}| \cos\phi} . \tag{5}$$

The dissipation factor is commonly expressed as

$$\tan(\delta) = \frac{1}{\omega R_P C_{DUT}} , \tag{6}$$

where $\delta = -\phi + 90°$.

III. RESULTS

A. Device under test—A multiferroic and magnetoelectric material

A suitable DUT for our experiment is a magnetoelectric material, where the electric and magnetic properties are strongly coupled. In this system, an external magnetic field changes the electric properties reflected as a change in capacitance through the changes both from dielectric constant[19,20] and dimensional change.[21,22]

In this report, we measured a high quality single crystal of $NiCo_2TeO_6$.[23,24] $NiCo_2TeO_6$ crystallizes in the noncentrosymmetric rhombohedral $R3$ structure and exhibits an incommensurate helical antiferromagnetic order with spins confined to the ab-plane. Its magnetic ordering occurs at around 52 K, and its magnetic propagation vector is determined as $k = [0, 0, 1.2109(1)]$. Notably, $NiCo_2TeO_6$ undergoes a hysteretic spin-flop transition at an external magnetic field of ~4 T. Dielectric anomalies coincide with its antiferromagnetic phase transition, and comprehensive terahertz and Raman spectroscopic studies reveal several low-frequency spin excitations—up to six distinct magnons at 5 K—that are highly sensitive to external magnetic fields, including the emergence of new modes and splitting near the spin-flop transition, which strongly indicate the presence of strong magnetoelectric coupling and electrically active electromagnons.[25]

B. Experimental data

In this measurement, the excitation voltage frequency is 101.01 kHz, and the sampling rate is 3.3333 MHz. The phase difference between the excitation voltage and the sample signal is clearly visible, primarily arising from the voltage amplifiers, the cables, and the impedance of the DUT, as shown in Fig. 3(b). To obtain accurate absolute values of the DUT's capacitance and dissipation, it is essential to account for phase shifts introduced by the voltage amplifiers and connecting cables. In our experiment, we measured the phase difference between voltage source and the DUT using an oscilloscope before inserting the probe into the cryostat. Similarly, we measured the phase shift between the other side of the DUT and the input of the current amplifier, as well as between the output of the current amplifier and the input of Voltage Amplifier 2. These measured phase shifts were subtracted during data processing to ensure accurate results.

C. Capacitance vs field

Figure 4 presents the magnetization, capacitance [Eq. (5)], and tan(δ) [Eq. (6)] of $NiCo_2TeO_6$ as a function of the magnetic field applied along the ab-plane. The oscillatory voltage excitation applies an electric field perpendicular to the ab-plane. These measurements were performed at 4 K over a magnetic field range from 0 to 50 T using the mid-pulse magnet.

In principle, the measured capacitance could be converted into the dielectric constant by assuming an infinite parallel plate capacitor geometry, given that the crystal is relatively thin compared to its lateral dimensions. The dielectric constant ϵ would then be given by
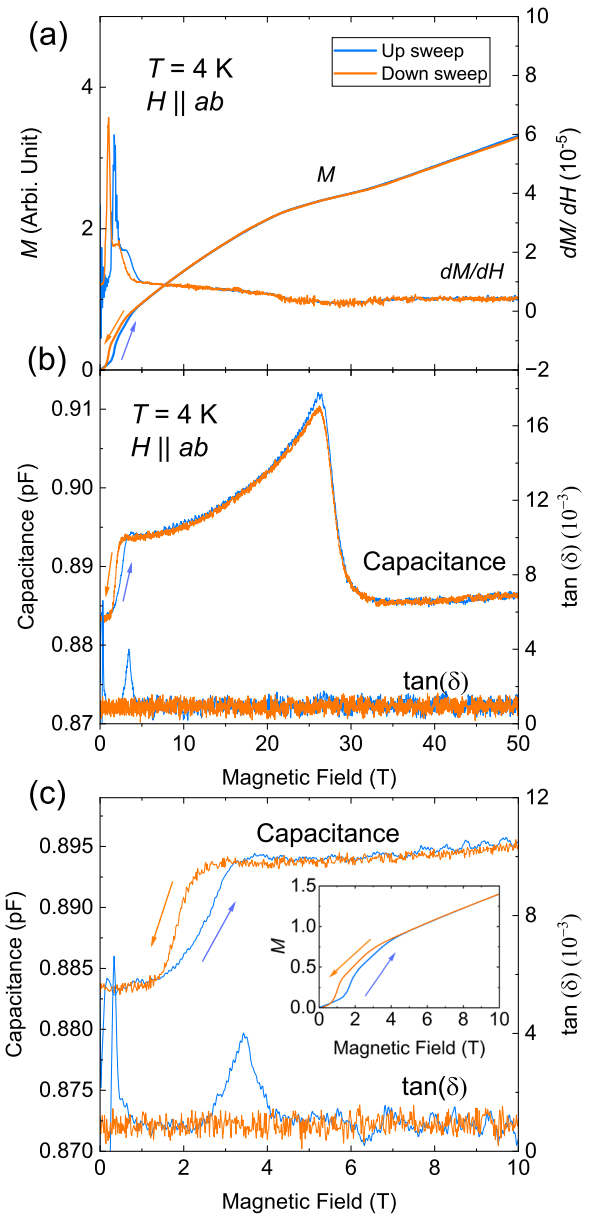
$$\epsilon = \frac{Cd}{A}, \quad (7)$$

FIG. 4. (a) Magnetic field dependence of magnetization and its susceptibility (dM/dH) for $NiCo_2TeO_6$ with the field applied along the ab-plane at 4 K. (b) Magnetic field dependence of capacitance and tan(δ), measured with the magnetic field along the ab-plane and the electric field perpendicular to the ab-plane, from 0 to 50 T at 4 K. (c) Enlarged view of the capacitance, tan(δ), and magnetization in the field range of 0–10 T.

where C is the capacitance, d is the thickness of the crystal, and A is the electrode area. In a high magnetic field, mechanical deformations or magnetostriction effects could alter these dimensions, introducing uncertainties in the extracted dielectric constant. For example, if the magnetostriction is ±100 ppm (see Ref. 9 for magnetostriction measurements in a similar material) then the ratio of d/A changes by

$\approx \pm 0.02\%$ for field perpendicular to the plane of the capacitor plates or $\approx \mp 0.01\%$ for field parallel to the plane of the capacitor plates.

As shown in Fig. 4(a), the magnetization exhibits a clear hysteresis loop between 0 and 4 T, which is more prominently highlighted in the inset of Fig. 4(c). Due to the steep changes in magnetization within this hysteresis region, the magnetic susceptibility (dM/dH) displays pronounced peaks, as shown in Fig. 4(a). Our capacitance measurements shown in Figs. 4(b) and 4(c) reveal a corresponding hysteresis near the same magnetic fields, indicating a strong magnetoelectric coupling in this compound. Interestingly, the tan(δ) data exhibit a pronounced peak during the upsweep of the magnetic field around 3.5 T, suggesting an energy dissipation process associated with the hysteresis loop. Note that the strong peak near the zero magnetic field is not from the DUT but caused by electrical noise generated at the beginning of the pulse, when the current through the magnet coil is largest. Another notable feature, albeit weaker, appears around 25 T as a subtle change in the slope of the magnetization curve. Remarkably, this weak change in magnetization coincides with a significant variation in capacitance, underscoring the sensitivity of capacitance measurements in detecting subtle magnetic state changes. This observation directly suggests that the weak slope change in magnetization near 25 T corresponds to a phase transition that is accompanied by an electrical phase transition.

More detailed analysis of the magnetization, capacitance, and electric polarization data, aimed at further elucidating the multiferroic and magnetoelectric coupling of this crystal, will be presented in a forthcoming publication.[24]

D. Comparison with commercial equipment

Figure 5 presents a comparison plot showing the capacitance and dissipation curves measured using a commercially available LCR meter (Keysight E4980A) in a DC field, alongside the pulsed field data obtained using the capacitance measurement technique developed in this study. The frequency, excitation voltage, and number of moving average points were 101 kHz, 1 V, and 6, respectively. While our technique measured capacitance values ~0.003 pF lower
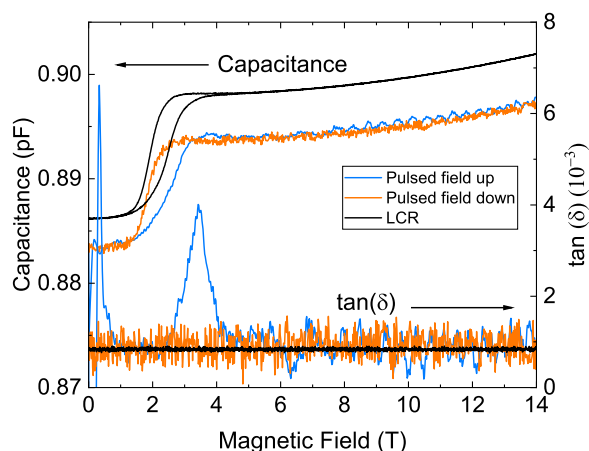
than those obtained with the LCR meter (less than 0.5%), the overall shape of the capacitance curve remained highly consistent between the two methods. Furthermore, the variation of capacitance as a function of the magnetic field showed excellent agreement between our technique and the LCR meter, confirming the reliability of our approach. The small discrepancy originates from a small signal distortion introduced by Voltage Amplifier 1, causing the sinusoidal waveform to become slightly triangular. This distortion leads to a slight underestimation of the amplitude in the Fourier transform analysis. The noise level in our measurements was determined to be ~0.001 pF. We anticipate that this noise can be reduced by an order of magnitude through data averaging, particularly by increasing the number of recorded data points. This suggests that with further optimization, our technique could achieve even greater precision in capacitance measurements. Although we do not present the higher frequency data here, we have confirmed that our measurement setup produces results consistent with those of the LCR meter up to 300 kHz.

For tan(δ), values obtained with both the LCR meter and our measurement technique (with a noise level of about 1×10^{-3}) were nearly identical. However, while no anomalies were observed in a DC magnetic field (with a maximum field sweep rate of 0.01 T/s), a pronounced peak emerged at around 3.5 T during pulsed field measurements, where the maximum sweep rate reached ~15 kT/s. If the observed hysteresis loop originates from changes in magnetic and electric domains, it is plausible that under a rapidly varying magnetic field, these domains undergo rapid reconfiguration to achieve equilibrium, resulting in significant energy dissipation. This suggests that the dissipation mechanism is highly sensitive to the field sweep rate, further supporting the strong coupling between magnetic and electric domain dynamics in this system.

Finally, we would like to address issues that can arise from environmental differences between DC and pulsed field measurements. A primary concern in pulsed field experiments is eddy current heating caused by the ultra-fast field sweep rate. Since the sample studied in this work is an insulator, we do not expect significant eddy current heating from the sample itself. However, eddy currents can arise if the metallic electrodes used for capacitance measurements are oriented perpendicular to the magnetic field. In our setup, the electrodes are aligned parallel to the field, effectively mitigating this effect. As a result, we believe any temperature rise due to eddy currents is negligible. Nevertheless, temperature variations arising from the sample's intrinsic magnetocaloric effect remain possible. To mitigate this, we introduced a sufficient amount of ^{4}He exchange gas (more than 100 mbar) to ensure good thermal coupling between the sample and its environment.

IV. CONCLUSION AND OUTLOOK

In this work, we have developed and implemented a capacitance measurement technique optimized for use in pulsed magnetic fields, demonstrating its capability to capture subtle magnetic and electric phase transitions. Our method shows excellent agreement with commercial LCR meters under DC field conditions while revealing unique features under extremely rapidly changing pulsed field environments. In particular, we observed a pronounced hysteresis in capacitance that aligns with magnetization measurements, confirming strong magnetoelectric coupling in NiCo$_2$TeO$_6$. In addition, the presence of a significant peak in tan(δ) under fast magnetic

FIG. 5. (a) Capacitance and tan(δ) measured by a commercially available LCR meter in DC field and capacitance and tan(δ) measured in a pulsed field with the same magnetic field and electric voltage configuration.

field sweeps suggests an energy dissipation process likely tied to rapid domain reconfiguration. These results highlight the advantage of our capacitance technique in detecting field-induced phase transitions that might otherwise remain elusive in conventional magnetization measurements.

Looking ahead, this capacitance measurement approach can be readily employed to enhance other experimental techniques. In particular, it is well-suited for general high-impedance measurements where minimizing leakage currents is critical. The setup developed in this study also offers a foundation for new measurement capabilities, such as capacitive torque magnetometry, magnetostriction detection, and magnetic-field-independent thermometry—enabling highly sensitive magnetocaloric and heat capacity measurements in pulsed magnetic fields. This approach thus opens new avenues for a comprehensive understanding of magnetoelectric interactions in complex materials. Its ability to resolve subtle changes in electronic and magnetic states under pulsed fields underscores its versatility, establishing it as a powerful tool for future high-field research. The potential applications extend beyond magnetoelectrics to a broad class of systems, including correlated electron materials, topological phases, and quantum phase transitions, offering fresh insight into emergent phenomena under extreme conditions.

ACKNOWLEDGMENTS

AUTHOR DECLARATIONS

Conflict of Interest

The authors have no conflicts to disclose.

Author Contributions

William K. Peria: Data curation (equal); Investigation (equal); Methodology (equal); Validation (equal); Writing – original draft (equal); Writing – review & editing (equal). **Shengzhi Zhang**: Data curation (equal); Investigation (equal). **Sangyun Lee**: Data curation (equal); Investigation (equal). **Gabriel Silva Freitas**: Data curation (equal); Investigation (equal). **Vivien S. Zapf**: Writing – review & editing (equal). **Choongjae Won**: Resources (lead). **Sang-Wook Cheong**: Resources (lead). **Minseong Lee**: Conceptualization (lead); Data curation (lead); Formal analysis (lead); Funding acquisition (lead); Investigation (lead); Methodology (lead); Project administration (lead); Resources (equal); Software (equal); Supervision (equal); Validation (lead); Visualization (lead); Writing – original draft (lead); Writing – review & editing (lead).

DATA AVAILABILITY

The data that support the findings of this study are available from the corresponding author upon reasonable request.

REFERENCES

[1] J. S. Xia, H. C. Choi, Y. Lee, and N. S. Sullivan, "Kapton capacitance thermometry at low temperatures and in high magnetic fields," J. Low Temp. Phys. **148**, 899 (2007).

[2] T. P. Murphy, E. C. Palm, L. Peabody, and S. W. Tozer, "Capacitance thermometer for use at low temperatures and high magnetic fields," Rev. Sci. Instrum. **72**, 3462 (2001).

[3] N. Anand, K. Barry, J. N. Neu, D. E. Graf, Q. Huang, H. Zhou, T. Siegrist, H. J. Changlani, and C. Beekman, "Investigation of the monopole magneto-chemical potential in spin ices using capacitive torque magnetometry," Nat. Commun. **13**, 3818 (2022).

[4] D. Martien, M. Williamsen, S. Spagna, R. Black, T. DaPron, T. Hogan, and D. Snow, "An ultrasensitive differential capacitive dilatometer," IEEE Trans. Magn. **55**, 6500204 (2019).

[5] J. P. Wampler, S. Liu, D. J. Mondal, M. Owczarek, S. Zhang, P. Wang, M. Gakiya-Teruya, M. Lee, H.-P. Cheng, M. Shatruk, and V. S. Zapf, "Magnetoelectric coupling in a Mn_4Na–organic complex under pulsed magnetic fields up to 73 T," J. Am. Chem. Soc. **146**, 32383 (2024).

[6] A. L. Blockmon, M. Lee, S. Zhang, Z. E. Manson, J. L. Manson, V. S. Zapf, and J. L. Musfeldt, "High field electrical polarization and magnetoelectric coupling in chiral magnet $[Cu(pym)(H_2O)_4]SiF_6 \cdot H_2O$," Inorg. Chem. **63**, 11737 (2024).

[7] M. Lee, R. Schönemann, H. Zhang, D. Dahlbom, T.-H. Jang, S.-H. Do, A. D. Christianson, S.-W. Cheong, J.-H. Park, E. Brosha *et al.*, "Field-induced spin level crossings within a quasi-XY antiferromagnetic state in $Ba_2FeSi_2O_7$," Phys. Rev. B **107**, 144427 (2023).

[8] K. D. Hughey, M. Lee, J. Nam, A. J. Clune, K. R. O'Neal, W. Tian, R. S. Fishman, M. Ozerov, J. Lee, V. S. Zapf, and J. L. Musfeldt, "High-field magnetoelectric and spin-phonon coupling in multiferroic $(NH_4)_2[FeCl_5 \cdot (H_2O)]$," Inorg. Chem. **61**, 3434 (2022).

[9] S. Zhang, S. Lee, A. J. Woods, W. K. Peria, S. M. Thomas, R. Movshovich, E. Brosha, Q. Huang, H. Zhou, V. S. Zapf, and M. Lee, "Electronic and magnetic phase diagrams of the Kitaev quantum spin liquid candidate $Na_2Co_2TeO_6$," Phys. Rev. B **108**, 064421 (2023).

[10] L. G. Rubin and P. A. Wolff, "High magnetic fields for physics," Phys. Today **37**(8), 24 (1984).

[11] M. Motokawa, "Physics in high magnetic fields," Rep. Prog. Phys. **67**, 1995 (2004).

[12] National Academies of Sciences, Engineering, and Medicine, *The current status and future direction of high-magnetic-field science and technology in the United States* (National Academies Press, 2024).

[13] F. Herlach, "Pulsed magnets," Rep. Prog. Phys. **62**, 859 (1999).

[14] D. N. Nguyen, J. Michel, and C. H. Mielke, "Status and development of pulsed magnets at the NHMFL pulsed field facility," IEEE Trans. Appl. Supercond. **26**, 4300905 (2016).

[15] J. Michel, D. N. Nguyen, and J. D. Lucero, "Design, construction, and operation of new duplex magnet at pulsed field facility-NHMFL," IEEE Trans. Appl. Supercond. **30**, 0500105 (2020).

[16] J. R. Michel, S. B. Betts, J. D. Lucero, A. Bhardwaj, L. N. Nguyen, and D. N. Nguyen, "Design and construction of the new 85T duplex magnet at NHMFL-Los Alamos," IEEE Trans. Appl. Supercond. **34**, 4900305 (2024).

[17] A. Miyake, H. Mitamura, S. Kawachi, K. Kimura, T. Kimura, T. Kihara, M. Tachibana, and M. Tokunaga, "Capacitive detection of magnetostriction, dielectric constant, and magneto-caloric effects in pulsed magnetic fields," Rev. Sci. Instrum. **91**, 105103 (2020).

[18] Keysight, *Impedance Measurement Handbook*, 6th ed. (Keysight, 2020).

[19]N. Hur, S. Park, P. A. Sharma, J. S. Ahn, S. Guha, and S.-W. Cheong, "Electric polarization reversal and memory in a multiferroic material induced by magnetic fields," Nature **429**, 392 (2004).

[20]T. D. Sparks, M. C. Kemei, P. T. Barton, R. Seshadri, E.-D. Mun, and V. S. Zapf, "Magnetocapacitance as a sensitive probe of magnetostructural changes in $NiCr_2O_4$," Phys. Rev. B **89**, 024405 (2014).

[21]X. Ding, Y.-S. Chai, F. Balakirev, M. Jaime, H. T. Yi, S.-W. Cheong, Y. Sun, and V. Zapf, "Measurement of the angle dependence of magnetostriction in pulsed magnetic fields using a piezoelectric strain gauge," Rev. Sci. Instrum. **89**, 085109 (2018).

[22]M. Jaime, C. Corvalán Moya, F. Weickert, V. Zapf, F. Balakirev, M. Wartenbe, P. Rosa, J. Betts, G. Rodriguez, S. Crooker, and R. Daou, "Fiber Bragg grating dilatometry in extreme magnetic field and cryogenic conditions," Sensors **17**, 2572 (2017).

[23]S. Skiadopoulou, M. Retuerto, F. Borodavka, C. Kadlec, F. Kadlec, M. Míšek, J. Prokleška, Z. Deng, X. Tan, C. Frank, J. A. Alonso, M. T. Fernandez-Diaz, M. Croft, F. Orlandi, P. Manuel, E. McCabe, D. Legut, M. Greenblatt, and S. Kamba, "Structural, magnetic, and spin dynamical properties of the polar antiferromagnets $Ni_{3-x}Co_xTeO_6$ ($x = 1, 2$)," Phys. Rev. B **101**, 014429 (2020).

[24]C. Won *et al.*, "High-field magnetoelectric coupling in $NiCo_2TeO_6$," (2025) (unpublished).

[25]A. Pimenov, A. A. Mukhin, V. Y. Ivanov, V. D. Travkin, A. M. Balbashov, and A. Loidl, "Possible evidence for electromagnons in multiferroic manganites," Nat. Phys. **2**, 97 (2006).

30 September 2025 18:22:38